IEEE Access
Multidisciplinary | Rapid Review | Open Access Journal

Received June 6, 2019, accepted June 23, 2019, date of publication July 3, 2019, date of current version July 22, 2019.

Digital Object Identifier 10.1109/ACCESS.2019.2926507

Weighted Tensor Nuclear Norm Minimization for Color Image Restoration

KAITO HOSONO[1], (Student Member, IEEE), SHUNSUKE ONO[2], (Member, IEEE), AND TAKAMICHI MIYATA[1], (Member, IEEE)

[1]Chiba Institute of Technology, Narashino 275-0016, Japan
[2]Department of Computer Science, School of Computing, Tokyo Institute of Technology, Tokyo 152-8552, Japan

Corresponding author: Kaito Hosono (s1122276hu@s.chibakoudai.jp)

This work was supported by the JSPS KAKENHI under Grant JP19K04377.

ABSTRACT Non-local self-similarity (NLSS) is widely used as prior information in an image restoration method. In particular, a low-rankness-based prior has a significant effect on performance. On the other hand, a number of color extensions of NLSS-based grayscale image restoration methods have been developed. These extensions focus on the pixel-wise correlation among color channels. However, a natural color image also has a complex dependency, known as an inter-channel dependency, among local regions from different color channels. As a result, color artifacts appear in a denoised image obtained by using the existing methods. In this paper, we propose a novel non-local and inter-channel dependency-aware prior called the weighted tensor nuclear norm (WTNN). The proposed prior is derived by incorporating inter-channel dependency to low-rank-based NLSS prior. The WTNN is a low-rankness-of-the-third-order patch tensor, and we apply it to the tensors constructed with non-local similar patches. It enables us to naturally represent the higher-order dependencies among similar color patches. We propose an image denoising algorithm using the WTNN and image restoration algorithm by using a non-trivial generalization of this algorithm. The experimental results clearly show that the proposed WTNN-based color image denoising and restoration algorithms outperform state-of-the-art methods.

INDEX TERMS Color image processing, image denoising, image restoration, nuclear norm, optimization, tensor.

I. INTRODUCTION

Color image restoration is a fundamental task in image processing that includes denoising, deblurring, inpainting, super-resolution, and compressed sensing restoration. Restoring a color image requires prior knowledge of the clean color image. Since we perform image restoration by casting into an optimization problem, such prior information needs to be represented as a *regularization function*. On the other hand, neural-network-based image restoration methods have been developed in recent years [1]–[3] and their restoration performance are competitive with state-of-the-art regularization-based methods. However, regularization-based methods still have the advantage in that their whole process can be explained explicitly.

Existing regularization-based image restoration methods are roughly classified into two classes by the prior information to be used: local methods [4]–[9] that use the intrinsic sparsity of natural images and non-local methods [10]–[18] that use their non-local self-similarity (NLSS). A local method uses only the surrounding areas to restore a target pixel, whereas a non-local method utilizes additional information from many regions, local and distant, that are similar to the target region. Non-local methods generally perform better than local methods.

Weighted nuclear norm minimization (WNNM) is a milestone work of a non-local grayscale image denoising that has been followed by many extension methods [19]–[21]. The method represents NLSS by using the weighted nuclear norm (WNN) of similar patch matrices. Each column of a matrix comprises the components of a local region in a grayscale image and similar non-local region. Since WNN approximates the rank function, we can use the WNN of a similar patch matrix to indicate similarities between similar patches.

Recently, many approaches for extending existing local methods for grayscale images to color (or multichannel) image restoration have been proposed [22]–[25].

The associate editor coordinating the review of this manuscript and approving it for publication was Shenghong Li.

However, only minor attention has been focused on extending non-local methods for color restoration [26]–[28]. These conventional non-local color image restoration methods usually use the *opponent color transform* (OPT) as a decorrelation process because the RGB channels of clean color images are highly correlated. Each color channel is restored separately after decorrelation. However, since the OPT is a pixel-wise operation, it is ineffective against complex dependencies among neighboring pixels from different color channels. As a result, color artifacts appear in a denoised image. We call this dependency *inter-channel dependency*, which cannot be captured by OPT.

In this paper, we propose a new NLSS and inter-channel dependency-aware prior called the *weighted tensor nuclear norm* (WTNN). Our key observation is that a low-rank-based non-local self-similarity prior can naturally handle inter-channel dependency because the prior is constructed from the local regions of a color image. The WTNN is designed to measure the non-local similarity and the inter-channel dependency simultaneously. In particular, we first construct third-order tensors by exploring the non-local similar patches from an input image. Then, we apply tensor unfolding to convert each tensor into three matrices. Interestingly, these matrices represent different aspects of the inter-channel dependency, and they are forecasted to be almost a low-rank in noiseless images.

The WTNN is a non-trivial generalization of the WNN, but is also a generalization of the *local color nuclear norm* (LCNN) [29], which is the image restoration method that uses inter-channel dependency and low rankness. The LCNN exploits inter-channel dependency by using the WNN of a local color matrix. Each column of a local color matrix consists of the component of each color channel of a local region. The LCNN minimizes the WNN of the local color matrix; a non-local extension of this process included as a part of the WTNN.

As the first application of our WTNN, we propose an efficient algorithm for color image denoising. We also propose a non-obvious extension of our denoising algorithm to the general image restoration problem, which includes the image denoising in its special case.

After finishing our work, we became aware of a state-of-the-art color image denoising method [30], which refers to our previous work [31], called the WTSTP (*weighted tensor Schatten p-norm and tensor ℓ_p-norm minimization*). In the WTSTP, a third-order input tensor is constructed by stacking all color channels of all similar patches into one direction, which means that the WTSTP is not a non-local generalization of LCNN, unlike the proposed WTNN. Furthermore, the WTSTP focuses on image denoising problems, whereas we propose an algorithm that can deal with general color image restoration problems.

This paper is organized as follows. Section II introduces some related works. Section III describes the notations and definitions. Section IV defines the WTNN and proposes its application to image denoising and image restoration. Section V compares our method with state-of-the-art restoration methods. Section VI concludes the paper.

The preliminary versions of this work without color image restoration have appeared in conference proceedings [31].

II. RELATED WORKS

A. GRAYSCALE IMAGE RESTORATION USING NON-LOCAL SIMILARITY

A NLSS is one of prior information of a natural image. A formulation of a non-local similarity has many approaches. In particular, low-rank approaches have been particular focus in recent years. The low-rank approaches measure a NLSS via the low rankness of a similar patch matrix, where each similar patch is restored by low-rank matrix approximations. However, such approximation is generally an NP-hard problem. Moreover, ideal similar patch matrices also require an ideal clean image.

Therefore, a WNNM was proposed as a state-of-the-art grayscale image denoising method. WNNM restores each similar patch by solving a minimization problem defined by the WNN instead of a low-rank matrix approximation. The denoising process of WNNM can be separated into three steps: 1) construction of similar patch matrices, 2) restoration of each patch, and 3) reconstruction of the image from each patch. WNNM can recover better similar patch matrices using an iteration of these processes.

B. COLOR IMAGE RESTORATION USING INTER-CHANNEL CORRELATION

Inter-channel correlation is prior information of a natural color image that is frequently used in color image restoration. That is, a correlation of each color channel represented by a color transform for decorrelation and restoration for each channel.

CBM3D is a color image denoising method that uses inter-channel correlation. This method is an extension of the *block matching 3D filtering* (BM3D), a non-local grayscale image denoising method that uses block matching (similar patch exploring) and 3D filtering (combination of 3D orthonormal transform and filtering). The algorithm of CBM3D executes two processes; color transform for an input image and BM3D denoising.

C. COLOR IMAGE RESTORATION USING INTER-CHANNEL DEPENDENCY

Inter-channel dependency is a prior information of a natural color image that differs from the inter-channel correlation. The LCNN [29] is a representation of an inter-channel dependency as the WNN of a local color matrix. A local image denoising method using LCNN with some conventional regularization functions can suppress color artifact. However, extending LCNN to a non-local method is not ovbious.

III. PRELIMINARIES

In what follows, let $\mathbb{N}$, $\mathbb{R}$ and $\mathbb{R}_+$ denote sets of all nonnegative integers, all real numbers, and all nonnegative real

numbers, respectively. We use small bold letters for column vectors, large bold letters for matrices, and large calligraphic letters for tensors.

We denote the set of *proper lower semicontinuous convex function* $\mathbb{R}^N \to \mathbb{R}$ as $\Gamma_0(\mathbb{R}^N)$. The *proximity operator* of $f \in \Gamma_0(\mathbb{R}^N)$ is defined as

$$\mathrm{prox}_f : \mathbb{R}^N \to \mathbb{R}^N : \mathbf{x} \mapsto \underset{\mathbf{y}\in\mathbb{R}^N}{\mathrm{argmin}} f(\mathbf{y}) + \frac{1}{2}\|\mathbf{x}-\mathbf{y}\|_2^2, \quad (1)$$

where $\|\cdot\|_2$ is the ℓ_2 norm (the Euclidian norm).

The indicator function with a convex set $S \subset \mathbb{R}^N$ is described as

$$\iota_S : \mathbb{R}^N \to \mathbb{R}\cup\{+\infty\} : \mathbf{x} \mapsto \begin{cases} 0 & (x \in S) \\ +\infty & (\text{otherwise}). \end{cases} \quad (2)$$

The WNN is defined as

$$\|\cdot\|_{\mathbf{w},*} : \mathbb{R}^{n_v\times n_h} \to \mathbb{R}_+ : \mathbf{X} \mapsto \sum_{k=1}^{n_m} w_k \sigma_k(X), \quad (3)$$

where $n_m = \min(n_v, n_h)$, $\sigma_k(X) \in \mathbb{R}_+ (k = 1, \cdots, n_m)$ is the k-th largest singular value of $\mathbf{X}$, and $\mathbf{w} = [w_1, \cdots, w_{n_m}]^\top \in \mathbb{R}_+^{n_m}$ is the weight vector that satisfies $0 \le w_1 < w_2 < \cdots < w_{n_m}$.

The proximity operator of the WNN cannot be defined because the WNN is usually a non-convex function. Therefore, we introduce the *pseudo proximity operator*, a non-convex case of Eq. (1). The pseudo proximity operator of the WNN $\mathrm{prox}_{\|\cdot\|_{\mathbf{w},*}}(\mathbf{X})$ can be characterized by the following minimization problem:

$$\min_{\mathbf{Y}\in\mathbb{R}^{n_v\times n_h}} \|\mathbf{Y}\|_{\mathbf{w},*} + \frac{1}{2}\|\mathbf{X}-\mathbf{Y}\|_F^2, \quad (4)$$

where $\|\cdot\|_F$ is the *Frobenius norm* (the Euclidian norm of a matrix). Prob. (4) has a closed form solution [32] as follows

$$\tilde{\mathbf{X}} = \mathbf{U}\mathrm{S}_{\mathbf{w}}(\Sigma)\mathbf{V}^\top, \quad (5)$$

where $\mathbf{X} = \mathbf{U}\Sigma\mathbf{V}^\top$ is the *singular value decomposition* (SVD) of $\mathbf{X}$, and $\mathrm{S}_{\mathbf{w}}(\Sigma)_{i,i} = \max(\Sigma_{i,i} - w_i, 0)$ is a weighted soft-thresholding operator.

In this paper, we assume that an observation model can be described as

$$\bar{\mathbf{y}} = \mathbf{A}\mathbf{x} + \mathbf{v}, \quad (6)$$

where $\bar{\mathbf{y}} \in \mathbb{R}^{3n}$, $\mathbf{A} \in \mathbb{R}^{3n\times 3n}$, $\mathbf{x} \in \mathbb{R}^{3n}$, and $\mathbf{v} \in \mathbb{R}^{3n}$ are an observation image (with n pixels and 3 color channels), a degradation matrix, an original image, and an additive white Gaussian noise with standard deviation σ_n, respectively. This observation model is a generalization of a popular image restoration model include inpainting, deblurring, and compressed sensing. For example, if $\mathbf{A}$ is a diagonal matrix with 0 or 1 diagonal elements, Eq. (6) is an observation model of an image inpainting problem.

The alternative direction method of multipliers (ADMM) [33] is an algorithm for solving the following convex optimization problem

$$\min_{\mathbf{u}\in\mathbb{R}^N, \mathbf{y}\in\mathbb{R}^{N'}} \{f(\mathbf{u}) + g(\mathbf{z})\} \quad \text{s.t. } \mathbf{z} = \mathbf{L}\mathbf{u}, \quad (7)$$

where $f \in \Gamma_0(\mathbb{R}^N)$, $g \in \Gamma_0(\mathbb{R}^{N'})$, and $\mathbf{L} \in \mathbb{R}^{N'\times N}$. For any $\mathbf{z}^{(0)}$, $\mathbf{d}^{(0)}$ and any $\rho > 0$, the iterative process of ADMM is given by **Algorithm** 1. ADMM is widely used in image restoration methods based on image prior information.

Algorithm 1 The Iterative Process of ADMM

Input: $\mathbf{z}^{(0)}$, $\mathbf{d}^{(0)}$, ρ

1: **while** *A stopping criterion is not satisfied* **do**
2: $\quad \mathbf{u}^{k+1} = \underset{\mathbf{u}}{\mathrm{argmin}} f(\mathbf{u}) + \frac{\rho}{2}\|\mathbf{z}^k - \mathbf{d}^k - \mathbf{L}\mathbf{u}\|_2^2$
3: $\quad \mathbf{z}^{k+1} = \mathrm{prox}_{\frac{1}{\rho}g}(\mathbf{L}\mathbf{u}^{k+1} + \mathbf{d}^k)$
4: $\quad \mathbf{d}^{k+1} = \mathbf{d}^k + \mathbf{L}\mathbf{u}^{k+1} - \mathbf{z}^{k+1}$
5: $\quad k = k + 1$
6: **end while**

Output: $\mathbf{u}^k$

IV. WEIGHTED TENSOR NUCLEAR NORM FOR IMAGE RESTORATION

A. DEFINITION OF WTNN

Let $\mathbf{y} \in \mathbb{R}^{3n}$ be a vectorized input color image. For the vectorized j-th local image patch ($R \times R$ pixels) of the s-th color channel $\mathbf{y}_{j,s} \in \mathbb{R}^{R^2} (s = 1, 2, 3)$ in input image $\mathbf{y}$, we can search for its M non-local similar patches $\mathbf{y}_{j,s}^{(l)} \in \mathbb{R}^{R^2} (l = 1, \cdots, M$ and $\mathbf{y}_{j,s}^{(1)} = \mathbf{y}_{j,s})$ in the large area around it on the basis of the Euclidian distance between patch vectors. Then, we stack those non-local similar patches into a third-order patch tensor $\mathcal{Y}_j \in \mathbb{R}^{R^2\times M\times 3}$. We denote this tensor as *similar patch tensor*. The flowchart of its construction is shown in Fig. 1.

Our proposed regularization function, named the *weighted tensor nuclear norm* (WTNN), is defined as

$$\|\cdot\|_{\mathbf{w},\boldsymbol{\gamma},*} : \mathbb{R}^{R^2\times M\times 3} \to \mathbb{R}_+ : \mathcal{X} \mapsto \sum_{m=1}^{3} \times \gamma_m \|\mathrm{unfold}_m(\mathcal{X})\|_{\mathbf{w}_m,*}, \quad (8)$$

where γ_m is the positive constant satisfying $\sum_m^3 \gamma_m = 1$, $\boldsymbol{\gamma} = [\gamma_1, \gamma_2, \gamma_3]^\top$,$\mathbf{w} = [\mathbf{w}_1^\top, \mathbf{w}_2^\top, \mathbf{w}_3^\top]^\top$, $\mathbf{w}_m$ is the weight vector of each WNN, and $\mathrm{unfold}_m(\cdot)$ is the *m-th mode tensor unfolding operator*. $\mathrm{unfold}_m(\cdot) : \mathbb{R}^{t_1\times\cdots\times t_N} \to \mathbb{R}^{t_m\times I_m}$ is defined as the map from tensor elements $(i_1, \cdots, i_N)$ to the corresponding matrix elements (i_m, j), where $I_m = \prod_{\substack{k=1\\k\neq m}}^{N} t_k$,

$$j = 1 + \sum_{\substack{k=1\\k\neq m}}^{N} (i_k - 1) \prod_{\substack{l=1\\l\neq m}}^{k-1} t_l. \quad (9)$$

B. APPLICATION TO COLOR IMAGE DENOISING

The color image denoising recovers an original color image $\mathbf{x} \in \mathbb{R}^{3n}$ from a corrupted observation

$$\bar{\mathbf{y}} = \mathbf{x} + \mathbf{v}, \quad (10)$$

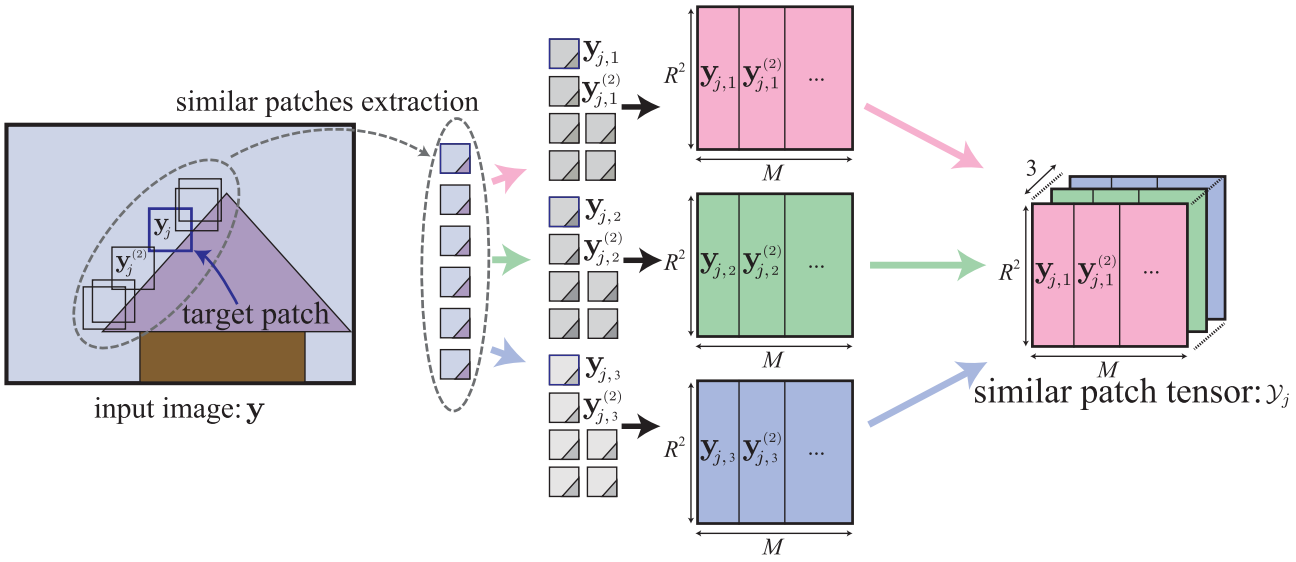

FIGURE 1. Construction of a patch tensor $\mathcal{Y}_j$ from an input image $\mathbf{y}$.

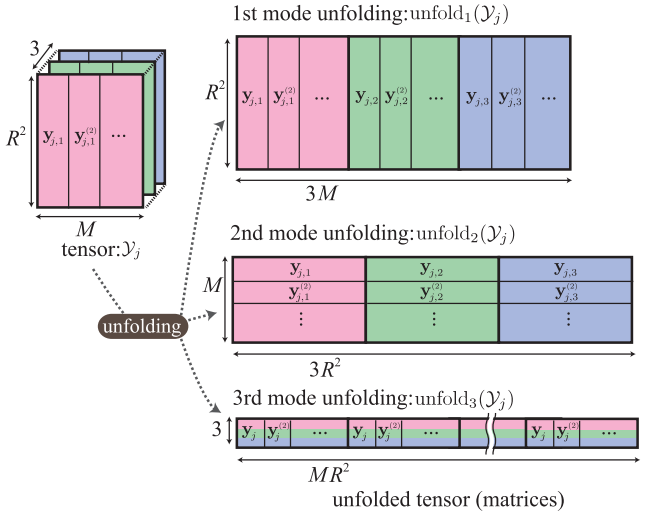

FIGURE 2. The operation of the tensor unfolding for the similar patch tensor.

where $\mathbf{v} \in \mathbb{R}^{3n}$ is an unknown additive white Gaussian noise with standard deviation σ_n. Please note that the model is a special case of Eq. (6) ($\mathbf{A} = \mathbf{I}$).

Since we expect the RGB color channels of a natural image to be highly correlated, we use the opponent color transform $\mathbf{C}$ as an (approximate) decorrelation transform before the denoising process. As we described above, despite the color transforms statistically decorrelating the color channels, transformed color channels still have inter-channel dependency, requiring them to be jointly processed.

We constructed similar patch tensors $\mathcal{Y}_j$ for the decorrelated input image $\mathbf{y} = \mathbf{C}\bar{\mathbf{y}}$. Thus, the obtained tensors satisfy $\mathcal{Y}_j = \mathcal{X}_j + \mathcal{V}_j$, where $\mathcal{X}_j$ and $\mathcal{V}_j$ are the similar patch tensors of an unknown original color image and an unknown additive white Gaussian noise, respectively.

By using the WTNN regularization, our color image denoising (i.e., estimating a clear patch tensor $\mathcal{X}_j$ from a corrupted patch tensor $\mathcal{Y}_j$) is formulated as the minimization problem

$$\min_{\mathcal{X}_j \in \mathbb{R}^{R^2 \times M \times 3}} \|\mathcal{X}_j\|_{\mathbf{w},\boldsymbol{\gamma},*} + \frac{1}{2}\|\mathcal{Y}_j - \mathcal{X}_j\|_2^2, \tag{11}$$

where $\|\cdot\|_2$ is the $\ell 2$ norm of a tensor defined as

$$\|\cdot\|_2 : \mathbb{R}^{R^2 \times M \times 3} \to \mathbb{R} : \mathcal{X} \mapsto \sqrt{\sum_{i=1}^{R^2}\sum_{j=1}^{M}\sum_{k=1}^{3}(\mathcal{X})_{i,j,k}^2}. \tag{12}$$

Eq. (11) is equivalent to the pseudo proximity operator of WTNN $\mathrm{prox}_{\|\cdot\|_{\mathbf{w},\boldsymbol{\gamma},*}}(\mathcal{Y}_j)$.

We use the weight setting proposed in [14] for our WTNN denoising. The weight vector $\mathbf{w}_m$ is determined as

$$(\mathbf{w}_m)_k = \sigma_n^2 c\sqrt{M}/(\hat{\sigma}_k(\mathbf{X}_{j,m}) + \epsilon), \tag{13}$$

where $c \in \mathbb{R}_+$ is a constant, $\epsilon = 10^{-16}$ is added to avoid dividing by zero, $\mathbf{X}_{j,m} = \mathrm{unfold}_m(\mathcal{X}_j)$, and $\hat{\sigma}_k(\mathbf{X}_{j,m})$ is the estimation of $\sigma_k(\mathbf{X}_{j,m})$ using the same estimation method in the implementation of the WNNM that is provided by the authors of [14].

The simple color image denoising algorithm using WTNN is thus described in **Algorithm** 2. However, the denoising performance of this algorithm is poor because of the difficulty of extracting similar patches due to the noise. Ideal similar patches could be obtained if the image was noiseless. However, there is intrinsically a *chicken-and-the-egg* problem because obtaining an ideal clean image also requires an ideal similar patches. Therefore, our denoising algorithm executes similar patch extraction and denoising on the basis of these patch clusters in an alternating manner. The same

Algorithm 2 Simple Color Image Denoising by WTNN

Input: Noisy image $\mathbf{y}$, Noise level σ_n

1: **for** Each patch $\mathbf{y}_j$ in $\mathbf{y}$ **do**
2: Extract similar patches from $\mathbf{y}$
3: Make similar patch tensor $\mathcal{Y}_j$
4: Determine weight vector $\mathbf{w}$ via Eq. (13)
5: Estimate $\mathcal{X}_j$ via Eq. (11)
6: Reconstruct $\hat{\mathbf{x}}$ from $\mathcal{X}_j$
7: **end for**

Output: Estimated image $\hat{\mathbf{x}}$

approach is generally used in non-local image denoising methods [10]–[18].

The proposed whole color image denoising algorithm is thus described in **Algorithm** 3. $\mathrm{D}^{\mathrm{WTNN}}(\mathbf{y}^{(p)}, \sigma_n^{(p)})$ is a simple color image denoising method described in **Algorithm** 2 for noisy image $\mathbf{y}^{(p)}$ and noise level $\sigma_n^{(p)}$. We apply the inverse opponent color transform $\mathbf{C}^{-1}$ at the end of our denoising algorithm to return a denoised image to RGB color space from an opponent color space.

Algorithm 3 Color Image Denoising by WTNN

Input: Noisy image $\bar{\mathbf{y}}$

1: Initialize $\mathbf{x}^{(0)} = \mathbf{C}(\bar{\mathbf{y}})$, $\mathbf{y}^{(0)} = \mathbf{C}(\bar{\mathbf{y}})$, $\sigma_n^{(0)} = \sigma_n$
2: **for** $p = 1 : P$ **do**
3: Iterative regularization $\mathbf{y}^{(p)} = \hat{\mathbf{x}}^{(p-1)} + \delta(\mathbf{y} - \hat{\mathbf{x}}^{(p-1)})$
4: **for** Each patch $\mathbf{y}_j$ in $\mathbf{y}^{(p)}$ **do**
5: **if** $p \neq 1$ **then**
6: Estimate local noise level $\sigma_n^{(p)} = \frac{\lambda \sigma_n^{(0)}}{r^2} \|\mathbf{y}_j - \hat{\mathbf{x}}_j^{(p-1)}\|_2^2$
7: **end if**
8: **end for**
9: Simple image denoising using WTNN $\hat{\mathbf{x}}^{(p)} = \mathrm{D}^{\mathrm{WTNN}}(\mathbf{y}^{(p)}, \sigma_n^{(p)})$
10: **end for**

Output: Estimated image $\mathbf{C}^{-1}(\hat{\mathbf{x}}^{(P)})$

Due to the similar patch extraction in **Algorithm** 3, we need to solve Prob. (11) several times for all similar patch tensors for the current estimated image. Because the unfolding operator was contained in WTNN, we need an operator splitting method (e.g., ADMM) to solve Prob. (11). However, such algorithms require a high computational cost because three SVD operations of an unfolded tensor are required for one iteration of these algorithms, making the entire color image denoising algorithm impractical. Therefore, we propose an inexact but computationally efficient solution to Prob. (11):

$$\mathcal{X}_j^* = \frac{1}{3} \sum_{m=1}^{3} \mathrm{refold}_m(\mathbf{U}_m \mathrm{S}_{\gamma_m \mathbf{w}_m}(\Sigma_m) \mathbf{V}_m^\top) \tag{14}$$

instead of using ADMM, where $\mathbf{Y}_{j,m} = \mathbf{U}_m \Sigma_m \mathbf{V}_m^\top$ is the SVD of $\mathbf{Y}_{j,m}$ and $\mathbf{Y}_{j,m} = \mathrm{unfold}_m(\mathcal{Y}_j)$.

C. APPLICATION TO COLOR IMAGE RESTORATION

Attempting to estimate the original image from the observation model Eq. (6) with $\mathbf{A} \neq \mathbf{I}$ is reffered to as color image restoration. Obtaining an efficient algorithm to achieve this means that we can solve many image restoration problems with only one algorithm by choosing appropriate $\mathbf{A}$.

Since $\mathbf{A} \neq \mathbf{I}$, decomposing the whole restoration process into patch-level processing and finding similar patches from the corrupted observation are infeasible. Thus, we cannot apply the color image denoising method shown in **Algorithm** 3 to solve general color image restoration problems.

On the other hand, the third line of the ADMM (shown in **Algorithm** 1) is a proximity operator. If Eqs. (1) and Eq. (11), and f is considered to be a regularization term, we can say that the proximity operator is corresponds to the denoising process. The assumption enables us to apply the ADMM in an unofficial manner to solve the WTNN-based color image restoration problem. This kind of approach is called the plug and play ADMM (PnPADMM) [34].

From these observations, we proposed a non-trivial extension of our denoising algorithm to solve the image restoration problem described as **Algorithm** 4.

Algorithm 4 Color Image Restoration by WTNN

Input: $\mathbf{y}$, $\mathrm{D}^{\mathrm{WTNN}}(\cdot)$, $\mathbf{A}$, ρ_1, ρ_2

1: **for** $k = 1 : K$ **do**
2: $\mathbf{u}^{k+1} = \underset{\mathbf{u}}{\mathrm{argmin}} f(\mathbf{u}) + \frac{\rho_2}{2} \|\mathbf{z}^k - \mathbf{d}^k - \mathbf{u}\|_2^2$
3: $\mathbf{z}^{k+1} = \mathrm{D}^{\mathrm{WTNN}}(\mathbf{u}^{k+1} + \mathbf{d}^k, \frac{\rho_1}{\rho_2})$
4: $\mathbf{d}^{k+1} = \mathbf{d}^k + \mathbf{u}^{k+1} - \mathbf{z}^{k+1}$
5: **end for**

Output: Restored image $\mathbf{u}^k$

The PnPADMM usually requires more than 100 iterations. Thus, we employ **Algorithm** 2 instead of **Algorithm** 3 as the denoiser in **Algorithm** 4. Since **Algorithm** 4 requires significant computational cost, using it as the denoiser in **Algorithm** 4 makes whole algorithm computationally unmanageble. We will show that the effectiveness of the PnPADMM using our simple denoising method in the next section.

V. EXPERIMENTAL RESULTS

A. COLOR IMAGE DENOISING

In this section, we verified our method's performance through numerical experiments. We used 12 natural color images (256×256 [pixel]) shown in Fig. 3 as original images. We added zero-mean additive white Gaussian noises with standard deviation σ_n (generated by using pseudo-random on Matlab 2018b) to those original images to generate observation images. The parameters of the proposed algorithm were set as in Table 1 for each noise level. The values of $\boldsymbol{\gamma}$ and c were chosen empirically, and the values of other parameters (R, M, P, σ, and λ) were the same as the default parameters of the published implementation of the WNNM [14].

FIGURE 3. 12 natural color images.

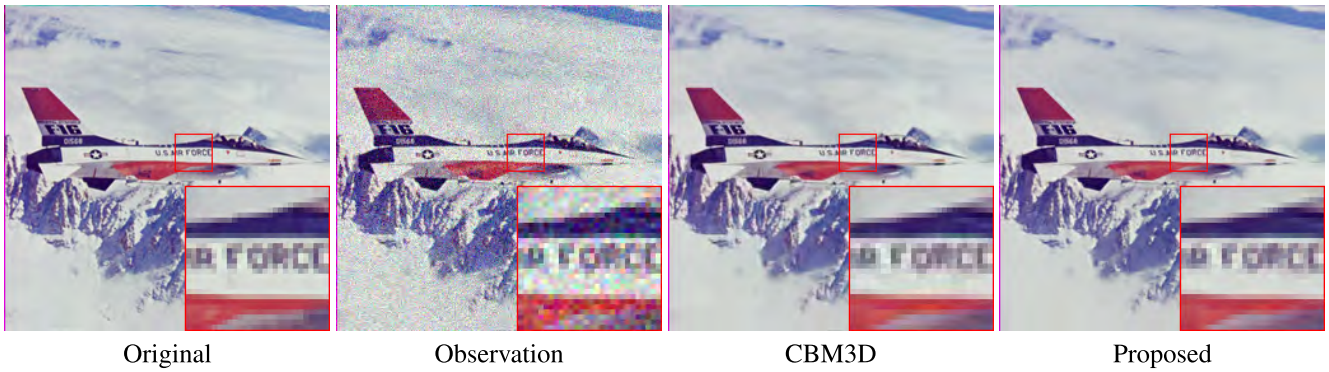

FIGURE 4. Denoised results of "Airplane," $\sigma_n = 20$.

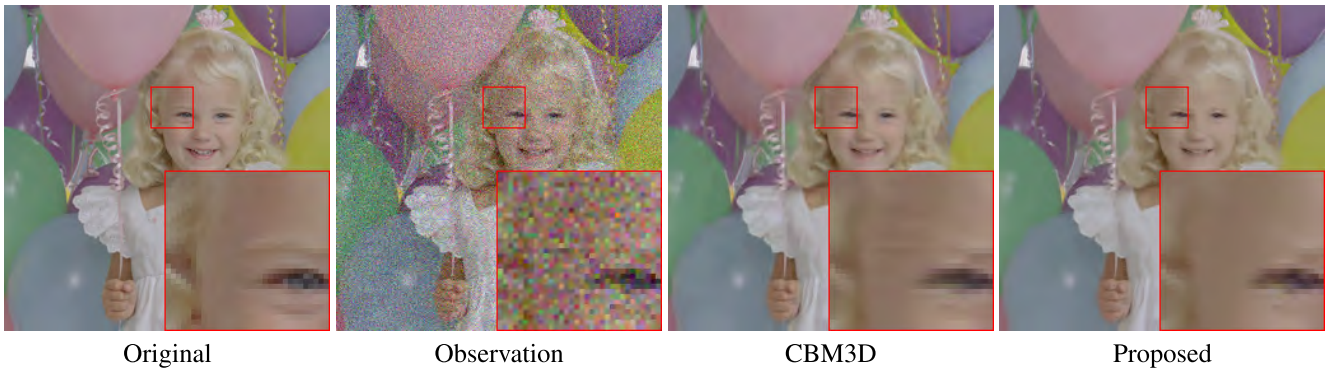

FIGURE 5. Denoised results of "Balloon," $\sigma_n = 20$.

TABLE 1. Parameters of proposed method in denoising experiments.

	$\sigma_n = 20$	$\sigma_n = 50$
γ	$\gamma_1 = 0.12, \gamma_2 = 0.1, \gamma_3 = 0.78$	
c	54.61	
R	6	8
M	70	120
P	8	14
δ	0.1	
λ	0.54	0.58

We compared the denoising performance of our proposed algorithm with CBM3D [26], a state-of-the-art color image denoising method that uses non-local similarity and color transform. Table 2 summarizes the PSNRs of denoised images by using the proposed method and CBM3D.

As shown in Table 2, our denoising algorithm outperformed CBM3D with the test images. Figs. 4, 5, 6, and 7 show four images from the denoising results. These results show that our method suppresses color artifacts more than CBM3D.

B. THE EFFECTIVENESS OF THE INEXACT SOLUTION

To analyze the effect of using the inexact solution Eq. (14) instead of solving Prob. (11) with ADMM, we compared denoised images obtained using inexact solution Eq. (14) and those obtained by exact solution Prob. (11) using ADMM. Hereafter, we call the formerly denoised images "inexact results" and the latter ones the "exact results." The parameters of ADMM were chosen as the number of iterations $N = 5$ and the step size parameters $\rho = 1$. As shown in Table 3, the denoising performances of these versions are quite similar. However, the averaged CPU time required to

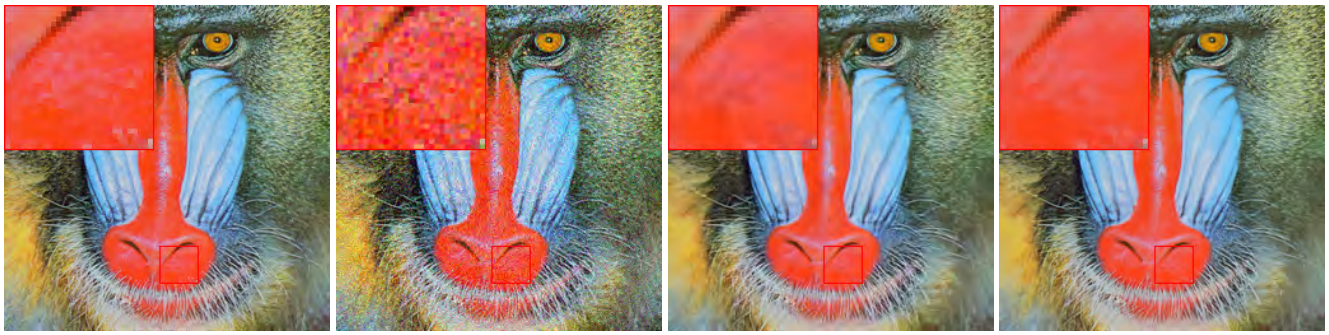

FIGURE 6. Denoised results of "Mandrill," $\sigma_n = 20$.

FIGURE 7. Denoised results of "milkdrop," $\sigma_n = 20$.

TABLE 2. Comparison of denoising performance of CBM3D and proposed method (PSNR[dB]).

σ_n	20		50	
Method	CBM3D	WTNNM	CBM3D	WTNNM
Aerial	28.08	**28.45**	24.28	**24.47**
Airplane	31.78	**32.62**	27.30	**27.88**
Balloon	34.46	**34.74**	**30.20**	30.19
Earth	32.24	**32.86**	28.01	**28.16**
Girl	32.19	**32.35**	**28.70**	28.60
Lenna	32.58	**33.04**	28.29	**28.64**
Mandrill	27.60	**28.12**	23.33	**23.77**
Parrots	33.62	**33.59**	28.90	**29.03**
Pepper	31.90	**32.52**	27.31	**27.92**
Sailboat	31.24	**31.89**	26.72	**27.25**
Couple	33.05	**33.12**	**29.13**	29.07
Milkdrop	34.73	**35.58**	30.20	**31.49**
Average	31.38	**31.83**	27.16	**27.51**

TABLE 3. Comparison of the inexact and the exact results in terms of PSNR[dB] and CPU time [sec] ($\sigma_n = 20$).

	Inexact	Exact
Aerial	28.46	28.48
Airplane	32.63	32.75
Balloon	34.85	34.90
Couple	33.35	33.27
Earth	32.88	33.08
Girl	32.48	32.42
Lenna	33.04	33.12
Mandrill	28.02	28.03
Milkdrop	35.68	35.73
Parrots	33.55	33.62
Pepper	32.57	32.60
Sailboat	31.95	32.00
Average	31.86	31.90
Average time	425.00	1946.00

produce the inexact results is almost five times shorter than that required to produce the exact results. These results show that the inexact solution Eq. (14) is a reasonable and effective solution.

C. COLOR IMAGE INPAINTING

In this section, we validate the effectiveness of our image restoration algorithm by comparing it with the PnPADMM that uses the CBM3D as a denoising function (PnPADMM + CBM3D).

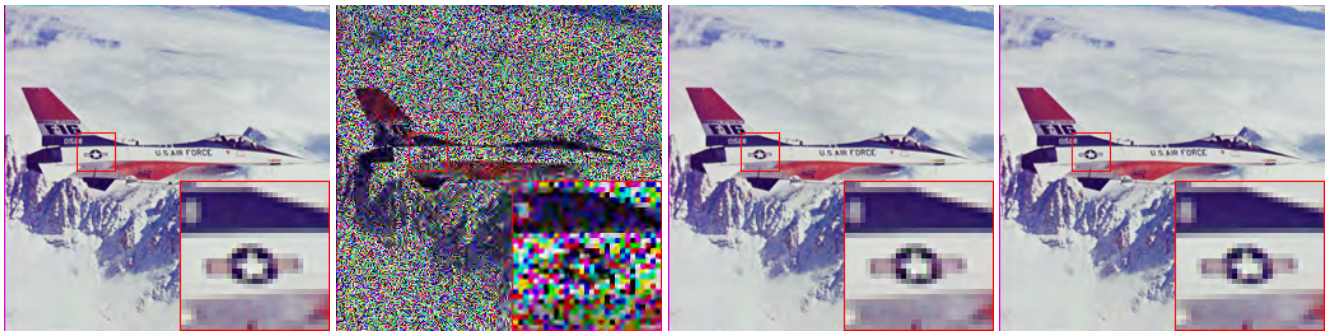

FIGURE 8. Inpainting results of "Airplane," missing rate is 40%.

TABLE 4. Parameters of simple denoising function in proposed algorithm.

γ	$\gamma_1 = 0.12, \gamma_2 = 0.1, \gamma_3 = 0.78$
c	30.06
R	5
M	60

TABLE 5. Inpainting performance comparison between PnPADMM + CBM3D and proposed method (PSNR [dB]).

Missing rate	20		40	
Method	CBM3D	WTNNM	CBM3D	WTNNM
Aerial	37.13	**37.95**	32.90	**33.34**
Airplane	42.81	**45.39**	38.18	**39.88**
Baloon	46.41	**47.84**	42.85	**43.45**
Earth	46.21	**48.79**	41.79	**43.14**
Girl	40.59	**41.17**	37.30	**37.52**
Lenna	43.87	**45.00**	39.54	**40.16**
Mandrill	35.79	**36.44**	31.35	**31.61**
Parrots	**47.08**	46.75	**41.38**	40.98
Pepper	42.12	**43.01**	37.94	**38.58**
Sailboat	43.44	**44.70**	38.55	**39.36**
Couple	42.31	**43.31**	38.87	**39.42**
Milkdrop	46.37	**48.82**	42.39	**44.49**
Average	42.84	**44.10**	38.59	**39.33**

We experimented with the 12 test images shown in Fig. 3 as original images. The goal of color image inpainting is to restore missing pixels. Missing of pixels are caused by object removal or sensor malfunction. The observation model of the image inpainting problem uses a diagonal matrix with 0 or 1 diagonal elements as a degradation matrix. We used a degradation matrix determined pseudo-randomly and depended on the missing rate as a degradation matrix $\mathbf{A}$. In this experiment, we assumed that the observation image was not corrupted with noise. Therefore, we chose $f(\mathbf{u}) = \iota_S(\mathbf{u})$ with $S = \{\mathbf{u} \in \mathbb{R}^{3n} \mid \mathbf{Au} = \mathbf{y}\}$.

The parameters of the PnPADMM for each method were set to $\rho_1 = 100$, $\rho_2 = 400$, and $K = 100$. Table 4 details the parameters of the denoising function of our method.

We compared the image inpainting performance of our method with PnPADMM + CBM3D. Table 5 shows that our method was more objectively effective. The inpainting result images shown in Fig. 8 show that the color artifact suppression performance of our method was higher than that of PnPADMM + CBM3D.

VI. CONCLUSION

In this paper, we proposed a novel color image non-local prior called the WTNN that we applied to the color image denoising method and the general color image restoration method. The WTNN can evaluate NLSS and inter-channel dependency simultaneously from a similar patch tensor. The tensor is constructed from a similar patch group searched for across an input color image.

In the color image denoising method, we introduced an inexact solution to the WTNN minimization method for reducing increased computational cost with an iterative algorithm. The experimental results showed the effectiveness of our WTNN-based image denoising method through comparing it to the CBM3D in terms of the quantitative and perceptual evaluation.

Furthermore, in the image restoration method, we proposed combining a WTNN-based simple color image denoising and the PnPADMM. We achieved a low computational cost by using a simple color image denoising algorithm instead of the whole color image denoising algorithm as a denoiser of the PnPADMM. The simple color image denoising is a non-iterative image denoising method that uses the WTNN. The experimental results exhibited the effectiveness of the proposed method in color image inpainting.

We will enable the automatic setting of our method's parameters in future work.

REFERENCES

[1] K. Zhang, W. Zuo, Y. Chen, D. Meng, and L. Zhang, "Beyond a Gaussian denoiser: Residual learning of deep CNN for image denoising," *IEEE Trans. Image Process.*, vol. 26, no. 7, pp. 3142–3155, Jul. 2017.

[2] T. Meinhardt, M. Moller, C. Hazirbas, and D. Cremers, "Learning proximal operators: Using denoising networks for regularizing inverse imaging problems," in *Proc. IEEE Int. Conf. Comput. Vis. (ICCV)*, Oct. 2017, pp. 1799–1808.
[3] D. Ulyanov, A. Vedaldi, and V. Lempitsky, "Deep image prior," in *Proc. IEEE Conf. Comput. Vis. Pattern Recognit. (CVPR)*, Jun. 2018, pp. 9446–9454.
[4] L. I. Rudin, S. Osher, and E. Fatemi, "Nonlinear total variation based noise removal algorithms," *Phys. D, Nonlinear Phenomena*, vol. 60, nos. 1–4, pp. 259–268, 1992.
[5] D. L. Donoho, "De-noising by soft-thresholding," *IEEE Trans. Inf. Theory*, vol. 41, no. 3, pp. 613–627, May 1995.
[6] C. Knaus and M. Zwicker, "Dual-domain image denoising," in *Proc. ICIP*, Sep. 2013, pp. 440–444.
[7] D. Zoran and Y. Weiss, "From learning models of natural image patches to whole image restoration," in *Proc. IEEE ICCV*, Nov. 2011, pp. 479–486.
[8] T. Blu and F. Luisier, "The SURE-LET approach to image denoising," *IEEE Trans. Image Process.*, vol. 16, no. 11, pp. 2778–2786, Nov. 2007.
[9] F. Luisier, T. Blu, and M. Unser, "A new SURE approach to image denoising: Interscale orthonormal wavelet thresholding," *IEEE Trans. Image Process.*, vol. 16, no. 3, pp. 593–606, Mar. 2007.
[10] K. Dabov, A. Foi, V. Katkovnik, and K. Egiazarian, "Image denoising by sparse 3-D transform-domain collaborative filtering," *IEEE Trans. Image Process.*, vol. 16, no. 8, pp. 2080–2095, Aug. 2007.
[11] J. Mairal, F. Bach, J. Ponce, G. Sapiro, and A. Zisserman, "Non-local sparse models for image restoration," in *Proc. ICCV*, Sep./Oct. 2009, pp. 2272–2279.
[12] W. Dong, L. Zhang, G. Shi, and X. Li, "Nonlocally centralized sparse representation for image restoration," *IEEE Trans. Image Process.*, vol. 22, no. 4, pp. 1620–1630, Apr. 2013.
[13] W. Dong, G. Shi, and X. Li, "Nonlocal image restoration with bilateral variance estimation: A low-rank approach," *IEEE Trans. Image Process.*, vol. 22, pp. 700–711, Feb. 2013.
[14] S. Gu, L. Zhang, W. Zuo, and X. Feng, "Weighted nuclear norm minimization with application to image denoising," in *Proc. CVPR*, Jun. 2014, pp. 2862–2869.
[15] J. Salvador, M. Borsum, and A. Kochale, "A Bayesian approach for natural image denoising," in *Proc. ICIP*, Sep. 2013, pp. 1095–1099.
[16] K. Dabov, A. Foi, V. Katkovnik, and K. Egiazarian, "BM3D image denoising with shape-adaptive principal component analysis," in *Proc. SPARS*, Apr. 2009, pp. 1–7.
[17] P. Chatterjee and P. Milanfar, "Patch-based near-optimal image denoising," *IEEE Trans. Image Process.*, vol. 21, no. 4, pp. 1635–1649, Apr. 2012.
[18] W. Zuo, L. Zhang, C. Song, D. Zhang, and H. Gao, "Gradient histogram estimation and preservation for texture enhanced image denoising," *IEEE Trans. Image Process.*, vol. 23, no. 6, pp. 2459–2472, Jun. 2014.
[19] J. Xu, L. Zhang, D. Zhang, and X. Feng, "Multi-channel weighted nuclear norm minimization for real color image denoising," in *Proc. ICCV*, Oct. 2017, pp. 1105–1113.
[20] Z. Zha, X. Yuan, B. Li, X. Zhang, X. Liu, L. Tang, and Y.-C. Liang, "Analyzing the weighted nuclear norm minimization and nuclear norm minimization based on group sparse sepresentation," Feb. 2017, *arXiv:1702.04463*. [Online]. Available: https://arxiv.org/abs/1702.04463
[21] Z. Zha, X. Zhang, Y. Wu, Q. Wang, X. Liu, L. Tang, and X. Yuan, "Non-convex weighted ℓ_p nuclear norm based ADMM framework for image restoration," *Neurocomputing*, vol. 311, pp. 209–224, Oct. 2018.
[22] X. Bresson and T. F. Chan, "Fast dual minimization of the vectorial total variation norm and applications to color image processing," *Inverse Problems Imag.*, vol. 2, no. 4, pp. 455–484, 2008.
[23] S. Ono and I. Yamada, "Decorrelated vectorial total variation," in *Proc. CVPR*, Jun. 2014, pp. 4090–4097.
[24] T. Miyata, "Inter-channel relation based vectorial total variation for color image recovery," in *Proc. ICIP*, Sep. 2015, pp. 2251–2255.
[25] J. Duran, M. Moeller, C. Sbert, and D. Cremers, "Collaborative total variation: A general framework for vectorial TV models," *SIAM J. Imag. Sci.*, vol. 9, no. 1, pp. 116–151, Jan. 2016.
[26] K. Dabov, A. Foi, V. Katkovnik, and K. Egiazarian, "Color image denoising via sparse 3D collaborative filtering with grouping constraint in luminance-chrominance space," in *Proc. ICIP*, Sep./Oct. 2007, pp. I-313–I-316.
[27] J. Mairal, M. Elad, and G. Sapiro, "Sparse representation for color image restoration," *IEEE Trans. Image Process.*, vol. 17, no. 1, pp. 53–69, Jan. 2008.
[28] J. Sun and Z. Xu, "Color image denoising via discriminatively learned iterative shrinkage," *IEEE Trans. Image Process.*, vol. 24, no. 11, pp. 4148–4159, Nov. 2015.
[29] S. Ono and I. Yamada, "Color-line regularization for color artifact removal," *IEEE Trans. Comput. Imag.*, vol. 2, no. 3, pp. 204–217, Sep. 2016.
[30] X. Zhang, J. Zheng, Y. Yan, L. Zhao, and R. Jiang, "Joint weighted tensor schatten p -norm and tensor ℓ_p -norm minimization for image denoising," *IEEE Access*, vol. 7, pp. 20273–20280, 2019.
[31] K. Hosono, S. Ono, and T. Miyata, "Weighted tensor nuclear norm minimization for color image denoising," in *Proc. ICIP*, Sep. 2016, pp. 3081–3085.
[32] K. Chen, H. Dong, and K.-S. Chan, "Reduced rank regression via adaptive nuclear norm penalization," *Biometrika*, vol. 100, no. 4, pp. 901–920, Sep. 2013.
[33] D. Gabay and B. Mercier, "A dual algorithm for the solution of nonlinear variational problems via finite element approximation," *Comput. Math. Appl.*, vol. 2, no. 1, pp. 17–40, 1976.
[34] S. H. Chan, X. Wang, and O. A. Elgendy, "Plug-and-play admm for image restoration: Fixed-point convergence and applications," *IEEE Trans. Comput. Imag.*, vol. 3, no. 1, pp. 84–98, Jan. 2017.

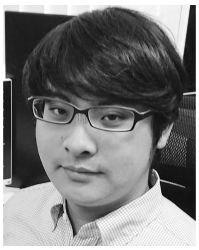

KAITO HOSONO (S'15) received the B.E. and M.E. degrees in engineering from the Chiba Institute of Technology, Chiba, Japan, in 2015 and 2017, respectively, where he is currently pursuing the Ph.D. degree with the Graduate School of Engineering. His current research interest includes image processing.

SHUNSUKE ONO (S'11–M'15) received the B.E. degree in computer science, and the M.E. and Ph.D. degrees in communications and computer engineering from the Tokyo Institute of Technology, in 2010, 2012, and 2014, respectively.

From 2012 to 2014, he was a Research Fellow (DC1) of the Japan Society for the Promotion of Science (JSPS). Since 2016, he has also been a Researcher with Precursory Research for Embryonic Science and Technology (PRESTO), Japan Science and Technology Corporation (JST), Tokyo, Japan. He is currently an Associate Professor with the Department of Computer Science, School of Computing, Tokyo Institute of Technology. His research interests include image processing, signal processing, mathematical optimization, and data science.

He received the Young Researchers' Award from the IEICE, in 2013, the Excellent Paper Award from the IEICE, in 2014, the Outstanding Student Journal Paper Award from the IEEE SPS Japan Chapter, in 2014, the Yasujiro Niwa Outstanding Paper Award from Tokyo Denki University, in 2015, the Seiichi Tejima Doctoral Dissertation Award from the Tokyo Institute of Technology, in 2016, the TELECOM System Technology Award from the Telecommunications Advancement Foundation, in 2016, and the Funai Research Award from the Funai Foundation, in 2017.

TAKAMICHI MIYATA (M'10) received the B.E. and M.E. degrees from the University of Toyama, in 2001 and 2003, respectively, and the Ph.D. degree from the Tokyo Institute of Technology, in 2006, where he joined as an Assistant Professor.

From 2012 to 2014, he was an Associate Professor with the Chiba Institute of Technology, where he has been a Professor, since 2014. His current research interest includes image processing. He received the Excellent Paper Award, in 2013, from the IEICE.